EUROGRAPHICS 2008 / Steve Marschner and Michael Wimmer
(Guest Editors)

Volume 27 (2008), Number 4

An Analysis of the In-Out BRDF Factorization for View-Dependent Relighting

Dhruv Mahajan, Yu-Ting Tseng and Ravi Ramamoorthi

Columbia University

Abstract

Interactive rendering with dynamic natural lighting and changing view is a long-standing goal in computer graphics. Recently, precomputation-based methods for all-frequency relighting have made substantial progress in this direction. Many of the most successful algorithms are based on a factorization of the BRDF into incident and outgoing directions, enabling each term to be precomputed independent of viewing direction, and re-combined at run-time. However, there has so far been no theoretical understanding of the accuracy of this factorization, nor the number of terms needed. In this paper, we conduct a theoretical and empirical analysis of the BRDF in-out factorization. For Phong BRDFs, we obtain analytic results, showing that the number of terms needed grows linearly with the Phong exponent, while the factors correspond closely to spherical harmonic basis functions. More generally, the number of terms is quadratic *in the frequency content of the BRDF along the reflected or half-angle direction. This analysis gives clear practical guidance on the number of factors needed for a given material. Different objects in a scene can each be represented with the correct number of terms needed for that particular BRDF, enabling both accuracy and interactivity.*

Categories and Subject Descriptors (according to ACM CCS): I.3.7 [Computer Graphics]: Three-Dimensional Graphics and Realism

1. Introduction

Real-time rendering of scenes with complex lighting, reflectance and changing view is a long-standing challenge in computer graphics. Recently, precomputed radiance transfer or PRT [SKS02] has shown great promise in achieving this goal, building on the seminal relighting work of [NSD94, DAG95]. In this paper, we focus on the class of all-frequency methods [NRH03], that seek to accurately reproduce intricate shadows and reflection effects, often using wavelet representations.

For view-dependent materials, a popular approach is to factor the BRDF into terms that depend only on incident and outgoing directions [LSSS04, WTL04].[†] This separable decomposition was originally proposed by [KM99] to represent BRDFs for real-time rendering. Each light transport term can then be precomputed for a static scene, independent of viewing direction, and combined interactively. Together with clustered PCA [SHHS03] to exploit signal coherence across different spatial locations, these methods for the first time enable real-time relighting of glossy objects with changing view.[‡] Since its introduction, the in-out BRDF factorization and variants have been used in most subsequent PRT papers [WTL05, WTL06, TS06, OBARG06, MKSRB07, SZC*07, WZH07, IDYN07].

It is possible to determine the number of terms needed for the in-out BRDF factorization directly by explicitly doing a SVD of the BRDF matrix, and looking numerically at

[†] Since the view is not known at precomputation, other factorizations like half and difference angles [Rus98] cannot be used for PRT.

[‡] An alternative approach of triple product integrals [NRH04], instead factors light transport into the visibility and BRDF. Since visibility and BRDF are in different spaces, it is not possible to exploit spatial coherence with CPCA, and real-time results are not easily achieved.

Published by Blackwell Publishing, 9600 Garsington Road, Oxford OX4 2DQ, UK and 350 Main Street, Malden, MA 02148, USA.

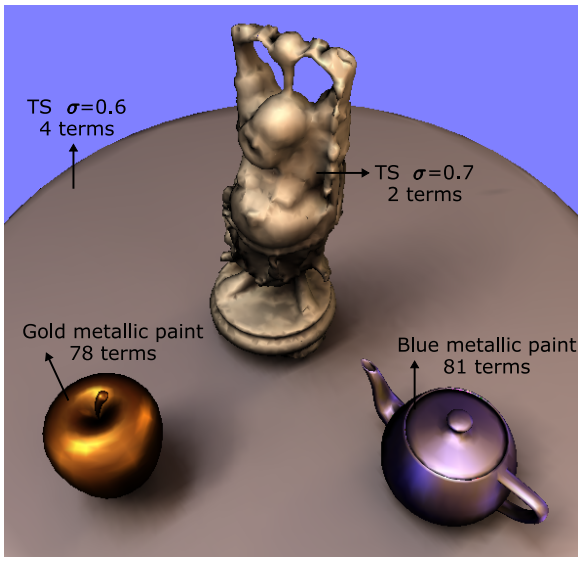

Figure 1: *A scene with a number of different view-dependent materials, rendered at interactive frame rates with in-out BRDF factorization and CPCA. The number of terms for each BRDF is chosen using our method, based on the theoretical analysis in the paper. As shown in the figure, more terms are needed for the high-frequency measured materials with sharp specular reflections. Closeups comparing to using a constant low number of terms, and to using the full BRDF (ground truth) are shown in Fig. 8.*

the falloff of eigenvalues. However, that does not confer insight nor generalize to different materials. Moreover, explicitly doing a SVD and choosing the number of terms can be expensive. This paper addresses these questions analytically and numerically.

For Phong BRDFs, we are able to analytically compute the factorization over the full sphere of directions, showing that the factors correspond closely to spherical harmonic basis functions.[§]

We generalize these results to Phong and other BRDFs limited to the visible hemisphere. A key result is that the number of terms needed is *linear* in the Phong exponent, and *quadratic* in the frequency content along the reflected or half-angle direction. One consequence is that a low-term factorization is accurate only for small to moderate glossiness. Practical guidance on numbers of terms needed is given for many common cases, allowing each material to be represented accurately with the correct number of BRDF terms (an example is shown in Fig. 1). Equivalently, our work leads to practical guidelines for what materials (how sharp a specular lobe) can be used, given a fixed computational budget or frame rate.

[§] Our analysis has some similarities to spherical harmonic convolution approaches [RH01], as well as analytic PCA decompositions of the light transport function [Ram02, MKSRB07], but is distinct in focusing on the BRDF. In [MKSRB07], the analysis is done in 2D and then extended by some empirical observations to 3D. In contrast, we provide precise and correct expressions for eigenvalues and eigenvectors for phong (or any radially symmetric) BRDF in 3D.

2. Background

For direct lighting, the reflection equation can be written as

$$B(\mathbf{x},\boldsymbol{\omega}_o) = \int_\Omega L(\boldsymbol{\omega}_i) V(\mathbf{x},\boldsymbol{\omega}_i) \rho(\boldsymbol{\omega}_i,\boldsymbol{\omega}_o)(\mathbf{n}(\mathbf{x})\cdot\boldsymbol{\omega}_i)\, d\boldsymbol{\omega}_i, \quad (1)$$

where B is the reflected light, L is the distant incident lighting, V is the (usually binary) visibility function, and ρ is the BRDF (with $\mathbf{n}$ the surface normal). $\boldsymbol{\omega}_i$ and $\boldsymbol{\omega}_o$ are the incident and outgoing angles. For view dependent relighting, it is common to factor the BRDF into a sum of terms, with each term being the product of factors in incident and outgoing directions $\boldsymbol{\omega}_i$ and $\boldsymbol{\omega}_o$,

$$\boxed{\rho(\boldsymbol{\omega}_i,\boldsymbol{\omega}_o) = \sum_{k=1}^{K} \sigma_k h_k(\boldsymbol{\omega}_o) g_k(\boldsymbol{\omega}_i),} \quad (2)$$

where σ_k are the singular values in a Singular Value Decomposition (SVD) of the BRDF. This allows us to precompute a transport function for each term

$$T_k(\mathbf{x},\boldsymbol{\omega}_i) = V(\mathbf{x},\boldsymbol{\omega}_i) g_k(\boldsymbol{\omega}_i)(\mathbf{n}(\mathbf{x})\cdot\boldsymbol{\omega}_i). \quad (3)$$

Note that T_k is now view-independent, and relighting reduces to

$$\begin{aligned} B(\mathbf{x},\boldsymbol{\omega}_o) &= \sum_{k=1}^{K} \sigma_k h_k(\boldsymbol{\omega}_o) \int L(\mathbf{x},\boldsymbol{\omega}_i) T_k(\mathbf{x},\boldsymbol{\omega}_i)\, d\boldsymbol{\omega}_i \\ &= \sum_{k=1}^{K} \sigma_k h_k(\boldsymbol{\omega}_o) \mathbf{T_k}\cdot\mathbf{L}, \end{aligned} \quad (4)$$

where the integral over incident directions $\boldsymbol{\omega}_i$ is typically reduced to a simple dot product $\mathbf{T_k}\cdot\mathbf{L}$ in a wavelet representation for environment map lighting. Equation 4 corresponds to the formulation introduced by [WTL04, LSSS04]. More recently, [WTL06] describe a simple extension, that uses the same BRDF factorization to also include interreflections.

In this paper, we analyze the BRDF factorization in equation 2 and the number of terms K needed. While our work is focused on PRT, the results also have fundamental implications for BRDF representation and analysis. Note that the final image accuracy ultimately depends on equation 4. However, since natural illumination has content at all frequencies, the accuracy of the BRDF filter is usually the limiting factor, and we therefore focus on equation 2. Actual examples rendered with PRT and complex lighting, that verify the theory developed in this paper, are shown in Figs. 1, 6 and 8.

3. Analysis for Phong BRDF

It is easiest for our analysis to start with the canonical Phong BRDF. We will see that in this case, we can derive analytic

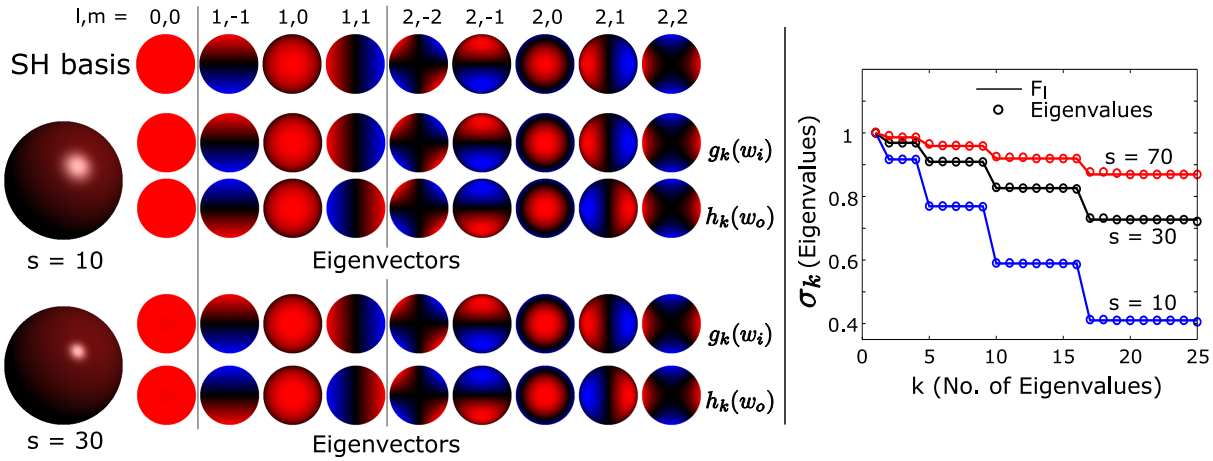

Figure 2: *Numerically computed eigenvectors and eigenvalues (same as singular values) for the BRDF matrix corresponding to Phong over the full sphere of directions. Leftmost, we show rendered spheres with exponents $s = 10$ and $s = 30$ (a small diffuse color is added here and in Fig. 3 only to aid in visualization). We show the eigenvectors $g_k(\boldsymbol{\omega}_i)$ and $h_k(\boldsymbol{\omega}_o)$ with red denoting positive values and blue denoting negative values, and see that they correspond to the spherical harmonic (SH) basis functions independent of exponent s (as predicted by the theory, the sign of h_k depends on $(-1)^m$). Rightmost, we show a graph of the numerically computed eigenvalues or singular values (circles) comparing to the theoretical predictions F_l (solid line), with excellent agreement.*

results that give considerable insight and indicate the number of terms needed. While exact analytic formulae are not available in other cases, the same insights hold for many other BRDF models.

We start by considering the normalized Phong BRDF,

$$\rho = \frac{s+1}{2\pi}(\mathbf{R}\cdot\mathbf{L})^s, \tag{5}$$

where s is the Phong exponent, $\mathbf{R}$ is the reflection of the view direction about the surface normal, and $\mathbf{L}$ is the light direction.

3.1. Spherical Harmonic Expansion

Much analytic insight is gained by considering the BRDF as defined over the full sphere (rather than only visible hemisphere) of incident and outgoing directions. Since the Phong lobe decays away from the reflected direction, this assumption does not significantly change the behavior of the model. Later in this section, we will explicitly consider the restriction to the visible hemisphere only.

We now proceed by expanding in spherical harmonics Y_{lm} [Mac48]. Since all BRDF values and numerical computations use real numbers, we use the real (as opposed to complex) form,

$$\begin{aligned} Y_{lm}(\theta,\phi) &= \sqrt{2}N_{lm}P_l^m(\cos\theta)\cos m\phi \quad m>0 \\ Y_{l0}(\theta,\phi) &= N_{lm}P_l^m(\cos\theta) \quad m=0 \\ Y_{lm}(\theta,\phi) &= \sqrt{2}N_{l|m|}P_l^{|m|}(\cos\theta)\sin|m|\phi \quad m<0, \end{aligned} \tag{6}$$

where (θ,ϕ) are spherical coordinates, N_{lm} is a normalization factor and P_l^m are the associated Legendre polynomials.

We now set $\cos\gamma = \mathbf{R}\cdot\mathbf{L}$, where γ is the angle between reflected and illumination directions. Then,

$$\rho = f(\gamma) = \sum_{l=0}^{\infty} f_l Y_{l0}(\gamma,\cdot), \tag{7}$$

where we use only the zonal harmonics $Y_{l0}(\gamma,\cdot)$ since the BRDF has no azimuthal dependence (is symmetric) when written in this way. Now, we invoke the spherical harmonic addition theorem,¶

$$\begin{aligned} Y_{l0}(\gamma,\cdot) &= \sqrt{\frac{4\pi}{2l+1}}\sum_{m=-l}^{l} Y_{lm}(\mathbf{R})Y_{lm}(\mathbf{L}) \\ &= \sqrt{\frac{4\pi}{2l+1}}\sum_{m=-l}^{l} Y_{lm}(\theta_o,\phi_o\pm\pi)Y_{lm}(\theta_i,\phi_i). \end{aligned} \tag{8}$$

The first line above is simply the statement of the spherical harmonic addition theorem. The second line uses the fact that the elevation and azimuthal angles for $\mathbf{R}$ are simply θ_o and $\phi_o \pm \pi$, and also inserts the incident angles (θ_i,ϕ_i) for $\mathbf{L}$. Finally, from the definitions in equation 6, it is clear that $Y_{lm}(\theta_o,\phi_o\pm\pi) = (-1)^m Y_{lm}(\theta_o,\phi_o)$. Applying this to the en-

¶ The complex form of the addition theorem is more commonly known, with the sum over $Y^*_{lm}(\mathbf{R})Y_{lm}(\mathbf{L})$, where Y^*_{lm} is the complex conjugate. It can be shown, by explicitly writing the complex harmonics in terms of real and imaginary parts, that this is equivalent to equation 8 for real harmonics.

tire BRDF, we obtain

$$\rho(\omega_i,\omega_o) = f(\gamma) = \sum_{l=0}^{\infty}\sum_{m=-l}^{l} F_l(-1)^m Y_{lm}(\theta_o,\phi_o)Y_{lm}(\theta_i,\phi_i), \tag{9}$$

where $F_l = f_l\sqrt{4\pi/(2l+1)}$. The reason for writing the spherical harmonic expansion in this way, is that it provides a *direct analytic factorization* into the form we seek with terms that depend only on $\boldsymbol{\omega}_o$ (i.e. $(-1)^m Y_{lm}(\theta_o,\phi_o)$) and only on $\boldsymbol{\omega}_i$ (i.e. $Y_{lm}(\theta_i,\phi_i)$).

3.2. SVD on Full Sphere

Consider the SVD decomposition of the Phong function, defined over the full sphere of directions (we will consider a restriction to the visible hemisphere, as required for physical BRDFs, shortly).

We simply write the BRDF in the form of equation 2, and identify the singular values σ_k as well as orthonormal basis functions g_k and h_k. Consider the form of equation 9, using a single index k to identify the terms (l,m). We can write $\sigma_k = F_l$, and $h_k(\boldsymbol{\omega}_o) = (-1)^m Y_{lm}(\theta_o,\phi_o) \quad g_k(\boldsymbol{\omega}_i) = Y_{lm}(\theta_i,\phi_i)$. The g_k and h_k are clearly orthonormal, since they are simply spherical harmonic basis functions. Therefore, by uniqueness of the SVD, *equation 9 directly represents the Singular Value Decomposition of the BRDF.*

To verify these results numerically, we constructed a BRDF matrix $\rho(\boldsymbol{\omega}_i,\boldsymbol{\omega}_o)$ using a resolution of $(40)^4$ in $(\theta_i,\phi_i,\theta_o,\phi_o)$. To preserve correct sampling on the sphere, we uniformly sampled along $\cos\theta$ and ϕ. We then computed the SVD using Matlab, and plotted eigenvectors and eigenvalues.[‖] Figure 2 shows our results. We can verify that the functions g_k and h_k are simply the spherical harmonics *independent of the Phong exponent s*. Moreover, the singular values or eigenvalues are simply F_l (these depend on s, since the decay of F_l is faster for smaller exponents). Note that each eigenvalue F_l is repeated $2l+1$ times because m ranges from $-l$ to $+l$.

3.3. Number of Terms Needed

These results enable us to easily determine the number of BRDF terms K needed for a given material. First, we must determine up to what frequency l^* we need to represent the BRDF accurately. Then, the number of terms

$$K = \left(l^*+1\right)^2. \tag{10}$$

Note that K is *quadratic in the frequency content* l^* of the BRDF, since there are $2l+1$ terms for each singular value F_l. We will see that this quadratic growth holds quite generally for many BRDFs.

[‖] For simplicity of exposition, we use the terms eigenvalues and eigenvectors loosely and interchangeably with the formally correct nomenclature of singular values and left/right singular vectors.

For Phong BRDFs, [RH01] have given an approximate formula for F_l as

$$F_l \approx \exp\left[-\frac{l^2}{2s}\right]. \tag{11}$$

One can use an appropriate threshold for how many terms are needed to preserve accuracy. A common very conservative threshold is for the spherical harmonic coefficients to decay so that $F_l \approx \exp[-3]$ which corresponds to $l^* \sim \sqrt{6s}$. Therefore, we have

$$K \approx 6s. \tag{12}$$

The number of terms grows *linearly* with the Phong exponent.

These results are verified numerically in Fig. 3, where we consider the number of terms needed for 99% accuracy for Phong BRDFs of increasing exponent s (Fig. 3A). It is seen that the number of terms needed grows linearly with the Phong exponent as expected (graph is a straight line), with 99% accuracy reached for $K \approx 5s$ (the value of $K = 6s$ in equation 12 is a bit too conservative). In the same figure, we show the effects of decreasing the number of terms used (Fig. 3B). In effect, this corresponds to fewer spherical harmonic coefficients and a lower-frequency BRDF. This is essentially similar to decreasing the Phong exponent—the result still looks like a glossy sphere, but is no longer accurate.

3.4. SVD on Hemispheres

In reality, the BRDF is defined (or non-zero) only over the visible hemispheres for incident and outgoing angles. Clamping it in this way can provide a more compact SVD with fewer terms. We emphasize that any rendered images (as in Figs. 3 and 4) will still consider the full sphere of normals; the restriction applies only to the BRDF matrix, where we restrict incident and outgoing angles (local light and view directions) to the physically valid visible hemisphere. A fully analytic factorization is no longer possible, but we can still derive and verify a number of significant results.

Most relevant to our analysis is the work of [MKSRB07], that explicitly considers the reduction in the number of eigenvalues when we go from a larger patch to a smaller one (in this case, the full sphere to a hemisphere). That analysis is based on the Szego eigenvalue theorem and its extension to the spherical domain [GS58, Oki96]. We will not repeat these rather technical details here, except for remarking that our example, with a mathematical form of $f(\mathbf{R}\cdot\mathbf{L})$ satisfies the relevant assumptions. The main result is that on the hemispherical domain, we will need approximately half the number of singular values for similar accuracy. The eigenmodes are no longer exactly spherical harmonics but still low-frequency basis functions.

This is validated numerically in Fig. 4, where we show the

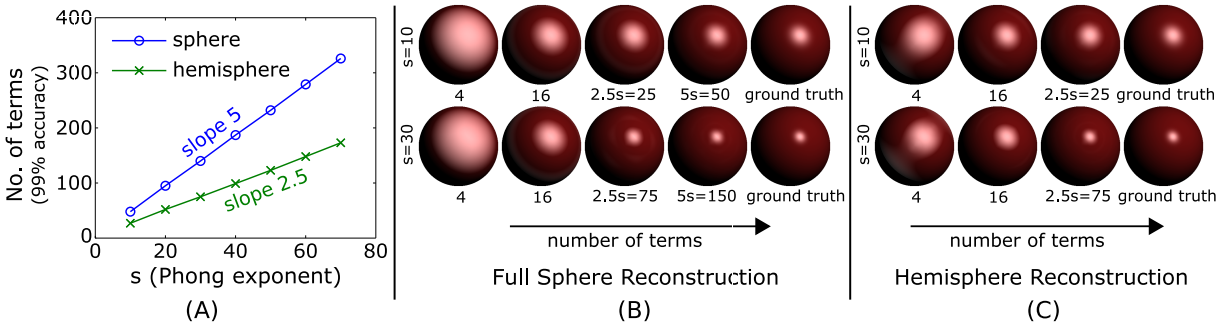

Figure 3: *Number of terms needed and accuracy for reconstructing the Phong BRDF over the full sphere and only the visible hemisphere.* ***A:*** *Number of terms for capturing 99% of the energy. The graph is clearly linear with Phong exponent, and number of terms* $\approx 5s$ *for SVD over the full sphere, and* $2.5s$ *when SVD is done over only the (physically valid) visible hemispheres.* ***B:*** *Accuracy of rendered images for different numbers of terms. Using fewer terms effectively corresponds to a lower frequency BRDF with smaller Phong exponent s. Using only 4 or 16 terms as in some previous works often does not suffice, and* $5s$ *terms are needed for high accuracy.* ***C:*** *Same as B when SVD is done only over the physical hemisphere. Half the number of terms* $2.5s$ *now suffices.*

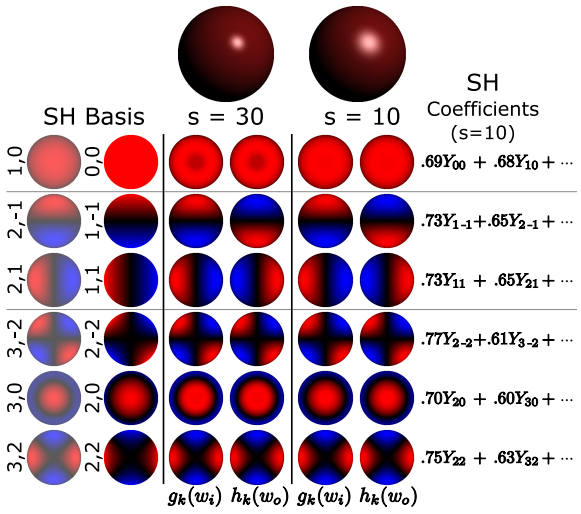

Figure 4: *Numerical eigenvectors for SVD of BRDF matrix, where incident and outgoing angles are restricted to the visible hemisphere of directions (compare to Fig. 2). The eigenmodes still correspond closely to spherical harmonic basis functions, but mix* Y_{lm} *with the same m. In general, dominant terms with* Y_{lm} *where* $l+m$ *is even are kept, while those with* $l+m$ *odd are incorporated into other eigenfunctions. The eigenvectors or factors* $g_k(\omega_i)$ *and* $h_k(\omega_o)$ *are still low frequency basis functions, largely similar (though not identical) for different Phong exponents s.*

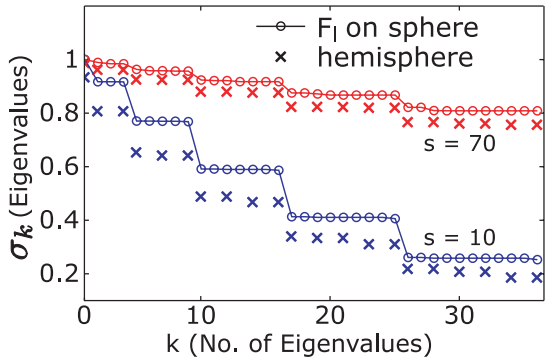

Figure 5: *Eigenvalues for SVD of BRDF matrix, where incident and outgoing angles are restricted to the visible hemisphere of directions. The solid line corresponds to* F_l *on the full sphere, but l is now the frequency on the hemisphere—note that there are now* $l+1$ *eigenvalues for given l, instead of* $2l+1$ *on the sphere. As expected from [Mahajan et al. 2007], the hemispherical and spherical eigenvalues are similar, but the number of terms needed for the hemispherical SVD is reduced to approximately half.*

SVD representation for a Phong BRDF with different exponents s, over the limited hemispherical domain. In fact, the low-frequency eigenmodes still closely correspond to some spherical harmonic basis functions (restricted to the hemisphere). More precisely, they are linear combinations of the Y_{lm}, where different l indices are somewhat mixed (but not the m indices, since that controls the variation with azimuthal angle ϕ, and remains orthogonal over the hemisphere). Interestingly, we observe that the dominant terms are still low-frequency harmonics, largely independent of the Phong exponent. However, the number of terms is approximately half of that for the spherical case at each level ($l+1$ instead of $2l+1$). In particular, terms with dominant Y_{lm} where $l+m$ is even are preserved, while those with $l+m$ odd are usually folded into other factors.

The eigenvalues are plotted in Fig. 5. The solid line corresponds to the spherical eigenvalues F_l as in the graph in

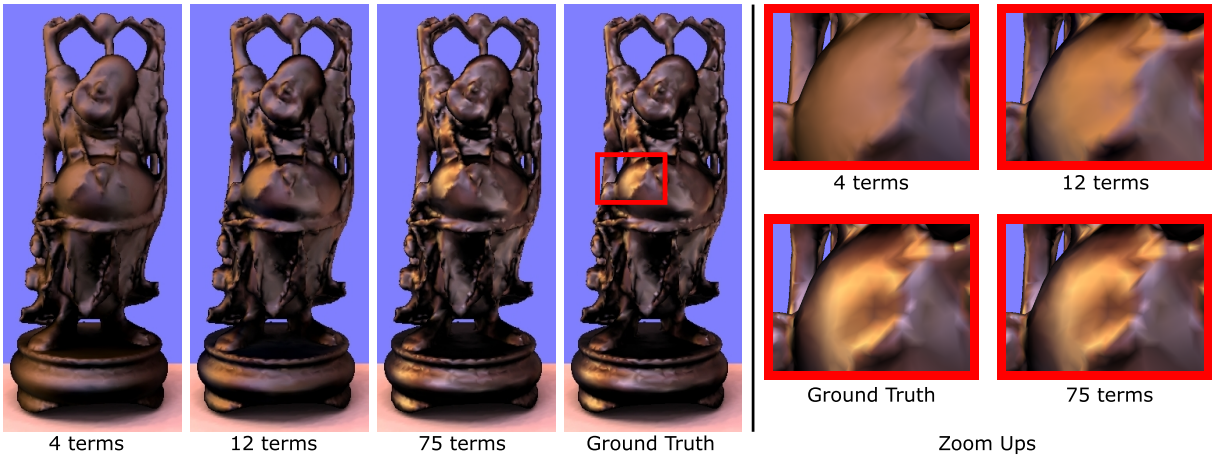

Figure 6: *Showing the effects of increasing the number of BRDF factors in complex lighting with an actual PRT rendering, for Phong exponent 30. Using 4 or 12 factors, as in some previous works, does not suffice in this case. As predicted by our theory, we need 75 terms here to accurately match ground truth images.*

Fig. 2, but the x-axis is scaled so that l is now the frequency for the hemispherical SVD (i.e. a given eigenvalue k corresponds approximately to eigenvalue $2k$ in Fig. 2 right). Notice that the spherical and hemispherical eigenvalues are approximately the same, but there are now $l+1$ (instead of $2l+1$) eigenvalues for frequency l. Hence, we verify that the number of eigenvalues needed for a given accuracy reduces to approximately half that for the SVD on the full sphere.

Regarding the number of terms needed, *K is still linear in the Phong exponent s and quadratic in the frequency content l^**, but we must now divide by a factor of 2,

$$\boxed{K \approx \frac{(l^*+1)^2}{2} \qquad K \approx \frac{5s}{2}.} \tag{13}$$

These results are verified numerically in Figs. 3A and 3C. The number of BRDF terms for 99% accuracy is linear in the Phong exponent s. Comparing to the spherical case in Fig. 3A, approximately half the terms are needed, i.e. $K \approx (2.5)s$ as expected. Similarly, Fig. 3C indicates that accuracy degrades as fewer terms are used, leading to the perception of a glossy material but with a much lower effective Phong exponent. These results are also consistent with those for the full sphere SVD in Figs. 3A and 3B.

Practical Implications: It is important to understand the practical consequences of these results for the types of BRDFs that can be used. A Phong BRDF of $s = 1$ requires $2-3$ terms for accurate representation. Most previous work has used at most $K = 16$ terms, which can give accurate results only for a low-frequency Phong BRDF with $s \approx 6$. (As seen in Fig. 3C, moderate Phong exponents like $s = 30$ cannot be represented accurately with 16 terms.) Most importantly, equation 13 provides immediate practical guidance as to the number of terms K to use for a given material. Equivalently, for a given K, it tells us what types of BRDFs (how sharp a specular lobe) we can accurately represent.

An example using an actual PRT system and environment map lighting is shown in Fig. 6, with Phong exponent $s = 30$. We see that increasing the number of BRDF terms more accurately captures the specularities. As expected $K \approx 2.5s = 75$ terms provides accurate results, and smaller numbers of terms blur the specular reflections. We chose drastically fewer terms for comparisons because these are the typical number of terms used in most of the current PRT methods. In general, the quality of the results increases smoothly with the number of terms. This is not surprising since our threshold is typically 99% of the energy, but other thresholds like 90% or 95% could as well be used.

4. General BRDFs

Completely analytic results are not easily derived for general BRDFs. However, we can make a number of observations. First, consider half-angle BRDF models like Blinn-Phong or Torrance-Sparrow with the simplified form

$$\rho = \frac{\exp\left[-\left(\frac{\cos^{-1}(\mathbf{N}\cdot\mathbf{H})}{\sigma}\right)^2\right]}{4\pi\sigma^2}. \tag{14}$$

In general, these models are a function of the angle between the normal $\mathbf{N}$ and half vector direction $\mathbf{H}$. For exitant angles far from grazing, it can be shown [RH01] that the spherical harmonic coefficients $F_l \approx \exp[-(\sigma l)^2]$.

The number of terms needed K is therefore proportional to $1/\sigma^2$. In fact, we find from Fig. 7C that $l^* \approx 1/(2\sigma^2)$ for σ ranging from 0.1-0.25 (the constant factors change somewhat, requiring higher l^* and more terms for larger σ). In practice, because of the relation between the half-angle and incident or reflected directions, we find that we need about half as many terms as for the equivalent Phong model with

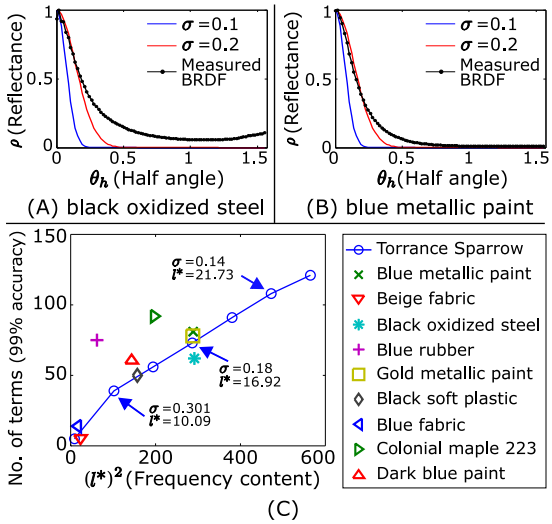

Figure 7: *Number of terms needed for general measured and analytic BRDFs. **A and B** show half-angle curves (dependence on θ_h) for two representative BRDFs from the Matusik database, along with reference Torrance-Sparrow curves. l^* can be found directly from these curves. **C** plots the number of terms K for 99% accuracy vs $(l^*)^2$ for Torrance-Sparrow BRDFs with different roughness σ, as well as for many measured materials. We verify that, in general, the number of terms K is quadratic in the frequency content l^*, or linear in $(l^*)^2$. Moreover, K for most measured materials is close to the line graph for Torrance-Sparrow, indicating the generality of our results for most BRDFs.*

dependence on the reflected direction, (i.e. $K \approx (l^*)^2/4$). Therefore, a rough surface BRDF with $\sigma = .2$ would need about 60 terms for accurate representation (many specular materials have σ in the range of $0.1 - 0.2$). A broad specular lobe of $\sigma = .4$ would still need about $K = 10 - 20$ terms.

These results can also be generalized to data-driven factorizations of BRDFs into functions of half and difference angles [LBAD*06]. In that case, one can determine l^* for the half-angle curve, and then use the analysis above to find the number of terms needed.

Practical Implications: The highest frequency components come from the specular 1D half-angle dependence, and a spherical harmonic transform can give us frequency l^* to a desired tolerance for measured data. For analytic BRDFs like Phong or Torrance-Sparrow, l^* can be computed from the formulae given earlier. Once we know the frequency content l^*, the number of terms will be *quadratic*, so that $K \sim (l^*)^2$ (actually for the half-angle dependence, $K \sim (l^*)^2/4$). This provides a general recipe for determining the number of terms needed for both analytic and measured BRDFs. The Phong BRDF results seen in Sec. 3 can be seen as a special case, where $l^* \approx \sqrt{6s}$, as noted above equation 12.

Figure 7 verifies these results using both analytic Torrance-Sparrow BRDFs, and a number of materials from the measured BRDF database of [MPBM03]. For the measured materials, we first computed the θ_h dependence by averaging BRDF values across different θ_d, omitting grazing angles where data is incomplete or noisy.** Some of our data-driven θ_h curves are shown in Figs. 7A and 7B, where we also show the Torrance-Sparrow model with σ = 0.1 and 0.2 for reference. From this data, we find l^* by a spherical harmonic transform. Figure 7C plots the number of terms K needed for many different measured materials and Torrance-Sparrow values of σ. As expected, $K \approx (l^*)^2/4$, with most measured BRDFs lying close to the line for Torrance-Sparrow.

Finally, Fig. 1 shows an actual result of using our method in PRT, on a scene of moderate complexity with 17,000 vertices. The number of BRDF terms is selected based on the analysis above, for both the measured materials and the Torrance-Sparrow BRDFs. As seen in the closeups in Fig. 8, simply using a constant low number of terms for all objects, as in most previous work, does not suffice for accurate results. At the same time, using a very large number of terms for all objects would slow performance below interactive rates. Our analysis enables the correct number of BRDF terms to be used for each object, with accurate real-time results.

5. Conclusions and Future Work

This paper has conducted a theoretical analysis of the In-Out BRDF factorization for view-dependent relighting, and validated it with extensive numerical simulations. We have shown that the number of terms needed grows *quadratically* with the frequency content of the BRDF, and *linearly* with the Phong exponent or equivalent.

These results make immediate practical contributions, since equation 13 gives a prescription for choosing the number of terms, as illustrated by PRT images shown in Figs. 1, 6 and 8. Equivalently, given a fixed budget, it tells us how to limit the specularity of materials in the scene. As examples of general guidance, a Phong exponent of $s = 1$ requires $2 - 4$ terms. A moderate Phong exponent of 20 would need about 50 BRDF factors. In practical applications where the number of terms K needs to be limited (to say $10 - 20$), only low frequency materials with $s < 10$ can be used accurately.

An interesting future direction is developing more compact factorizations for higher performance (using fewer terms K). This line of work is especially challenging because

** For this figure, we averaged across the RGB colors, but it is also possible to simply treat the three color channels separately as in our renderings.

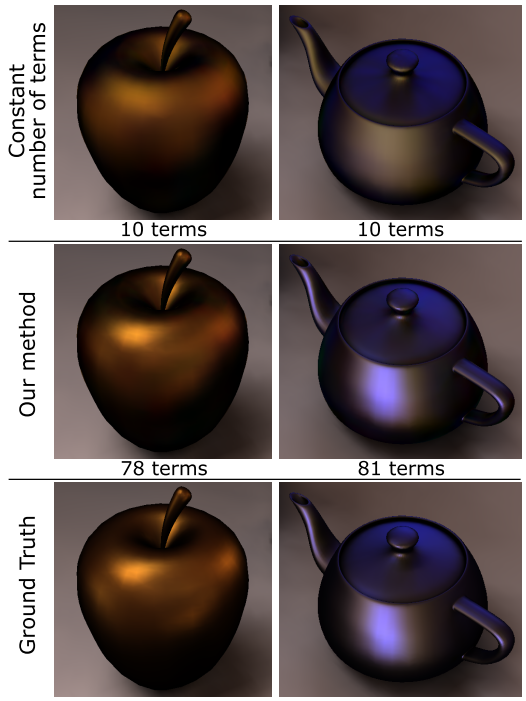

Figure 8: *Closeups of the apple and teapot from Fig. 1. Using a constant small number of 10 terms in the BRDF factorization, as in some previous methods, is insufficient to reproduce high-frequency specularities, while using the number of terms predicted by our method provides accurate results. Our method allows one to choose the required number of terms separately for each object, with fewer terms required for the lower-frequency materials in Fig. 1 (table and Buddha), and more for the objects shown here.*

the requirement of view-independence for one of the BRDF factors precludes alternatives like half and difference angles. More broadly, we may consider general solutions to the difficult problem of all-frequency light and view manipulation for highly specular materials. The main alternative is the use of triple product integrals [NRH04]. In that work however, visibility and BRDF are factored and represented in different spaces. This makes it very hard to exploit spatial coherence using methods like CPCA, which are needed for real-time performance. Thus, there remain fundamental challenges to view-dependent relighting (how to exploit spatial coherence in triple products, or how to more efficiently factor BRDFs).

Much of the recent progress in PRT is based on a number of clever approximations and factorizations that give pleasing visual results. However, the accuracy of these approximations is often not clearly understood. With the growing maturity of the field, it is critical to develop a firm mathematical foundation by conducting a careful theoretical and empirical analysis of common approximations, and we see this paper as an important step in that direction.

Acknowledgements

This work was supported in part by the NSF (grants CCF 03-05322, IIS 04-30258, CCF 04-46916, CCF 07-01775), a Sloan Research Fellowship, and an ONR Young Investigator award N00014-07-1-0900.

References

[DAG95] DORSEY J., ARVO J., GREENBERG D.: Interactive design of complex time-dependent lighting. *IEEE Computer Graphics and Applications 15*, 2 (1995), 26–36.

[GS58] GRENANDER U., SZEGO G.: *Toeplitz Forms and Their Applications*. University of Calif. Press, Berkeley and Los Angeles, 1958.

[IDYN07] IWASAKI K., DOBASHI Y., YOSHIMOTO F., NISHITA T.: Precomputed radiance transfer for dynamic scenes taking into account light interreflection. In *EuroGraphics Symposium on Rendering* (2007), pp. 35–44.

[KM99] KAUTZ J., MCCOOL M.: Interactive rendering with arbitrary BRDFs using separable approximations. In *EuroGraphics Symposium on Rendering* (1999), pp. 247–260.

[LBAD*06] LAWRENCE J., BEN-ARTZI A., DECORO C., MATUSIK W., PFISTER H., RAMAMOORTHI R., RUSINKIEWICZ S.: Inverse shade trees for non-parametric material representation and editing. *ACM Transactions on Graphics (SIGGRAPH 2006) 25*, 3 (2006), 735–745.

[LSSS04] LIU X., SLOAN P., SHUM H., SNYDER J.: All-frequency precomputed radiance transfer for glossy objects. *EuroGraphics Symposium on Rendering 2004* (2004), 337–344.

[Mac48] MACROBERT T.: *Spherical harmonics: an elementary treatise on harmonic functions with applications*. Dover Publications, 1948.

[MKSRB07] MAHAJAN D., KEMELMACHER-SHLIZERMAN I., RAMAMOORTHI R., BELHUMEUR P.: A theory of locally low dimensional light transport. *ACM Transactions on Graphics (SIGGRAPH 2007) 26*, 3 (2007), 62.

[MPBM03] MATUSIK W., PFISTER H., BRAND M., MCMILLAN L.: A data-driven reflectance model. *ACM Transactions on Graphics (SIGGRAPH 2003) 22*, 3 (2003), 759–769.

[NRH03] NG R., RAMAMOORTHI R., HANRAHAN P.: All-frequency shadows using non-linear wavelet lighting approximation. *ACM Transactions on Graphics (SIGGRAPH 2003) 22*, 3 (2003), 376–381.

[NRH04] NG R., RAMAMOORTHI R., HANRAHAN P.: Triple product wavelet integrals for all-frequency relighting. *ACM Transactions on Graphics (SIGGRAPH 2004) 23*, 3 (2004), 475–485.

[NSD94] NIMEROFF J., SIMONCELLI E., DORSEY J.: Efficient re-rendering of naturally illuminated environments. In *EuroGraphics Workshop on Rendering* (1994), pp. 359–373.

[OBARG06] OVERBECK R., BEN-ARTZI A., RAMAMOORTHI R., GRINSPUN E.: Exploiting temporal coherence for incremental all-frequency relighting. In *EuroGraphics Symposium on Rendering* (2006), pp. 151–160.

[Oki96] OKIKIOULU K.: The analogue of the strong Szego limit theorem on the 2- and 3- dimensional spheres. *Journal of the American Mathematical Society 9*, 2 (1996), 345–372.

[Ram02] RAMAMOORTHI R.: Analytic PCA construction for theoretical analysis of lighting variability in images of a lambertian object. *IEEE PAMI 24*, 10 (2002), 1322–1333.

[RH01] RAMAMOORTHI R., HANRAHAN P.: A signal processing framework for inverse rendering. *In Proceedings of SIGGRAPH (2001)* (2001), 117–128.

[Rus98] RUSINKIEWICZ S.: A new change of variables for efficient BRDF representation. In *EuroGraphics Symposium on Rendering* (1998), pp. 11–22.

[SHHS03] SLOAN P., HALL J., HART J., SNYDER J.: Clustered principal components for precomputed radiance transfer. *ACM Transactions on Graphics (SIGGRAPH 2003) 22*, 3 (2003), 382–391.

[SKS02] SLOAN P., KAUTZ J., SNYDER J.: Precomputed radiance transfer for real-time rendering in dynamic, low-frequency lighting environments. *ACM Transactions on Graphics (SIGGRAPH 2002) 21*, 3 (2002), 527–536.

[SZC*07] SUN X., ZHOU K., CHEN Y., LIN S., SHI J., GUO B.: Interactive relighting with dynamic BRDFs. *ACM Transactions on Graphics (SIGGRAPH 2007) 26*, 3 (2007), 27.

[TS06] TSAI Y., SHIH Z.: All-frequency precomputed radiance transfer using spherical radial basis functions and clustered tensor approximation. *ACM Transactions on Graphics (SIGGRAPH 2006) 25*, 3 (2006), 967–976.

[WTL04] WANG R., TRAN J., LUEBKE D.: All-frequency relighting of non-diffuse objects using separable BRDF approximation. In *EuroGraphics Symposium on Rendering* (2004), pp. 345–354.

[WTL05] WANG R., TRAN J., LUEBKE D.: All-frequency interactive relighting of translucent objects with single and multiple scattering. *ACM Transactions on Graphics (SIGGRAPH 2005) 24*, 3 (2005), 1202–1207.

[WTL06] WANG R., TRAN J., LUEBKE D.: All-frequency relighting of glossy objects. *ACM Transactions on Graphics 25*, 2 (2006), 293–318.

[WZH07] WANG R., ZHU J., HUMPHREYS G.: Precomputed radiance transfer for real-time indirect lighting using a spectral mesh basis. In *EuroGraphics Symposium on Rendering* (2007).